Radiated energy evolution during seismic sequences

Stefania Gentili

Radiated energy evolution during seismic sequences

S. Gentili

Istituto Nazionale di Oceanografia e di Geofisica Sperimentale, Centro Ricerche Sismologiche, Via Treviso 55, 33100 Cussignacco, Udine, Italy. Tel. +39 040 2140134, Fax. +39 0432 522474

E-mail: sgentili@inogs.it

Keywords: Omori law, Gutenberg Richter law, seismic sequences, c value estimation, energy evolution, parameters correlation

Abstract

In this paper, I propose a new equation describing the evolution of seismic sequences, based on radiated energy. The evolution of radiated energy in time is described as function of the *p* and *c* parameters of the modified Omori law and of the energy radiated within a short time following the mainshock. By using the energy rather than the number of events in describing seismic sequences, I circumvent the problem of missing weak aftershocks close in time to the mainshock, because most of the total energy is contained in largest events. In addition, I propose an equation describing the difference in magnitude between the mainshock and the strongest aftershock as function of the energy radiated in a short time after the mainshock, of *p*, *c*, and of the parameter *b* of the Gutenberg Richter equation. An application to California sequences shows values of *p* in the range [0.65, 1.5] and *c* in the range [0, 0.25] and no dependence of *c* on the difference between mainshock and cutoff magnitude.

1. Introduction

Seismic sequences have been studied since the end of the 19th century to find general laws describing their time evolution and energy distribution. The so called "Båth law", anticipated by Richter (1958) and then presented in larger detail by Båth (1965), states that the sample mean of the difference Δm between the mainshock and the strongest aftershock magnitudes is 1.2, for magnitudes based on surface wave scale. However, Båth (1965) itself provided examples in which the Båth law does not hold. Compatible results were found by Utsu (1957, 1961) on Japanese catalogue. This approach does not consider the different productivity and magnitude distribution from one sequence to the other and the temporal distribution of aftershocks.

In the same years, despite considerable statistical variability associated with seismicity, important general laws were observed for seismic sequences, like the Modified Omori Law (MOM – Utsu, 1961) the frequency-magnitude scaling (Gutenberg and Richter, 1954) and, subsequently, the Reasenberg and Jones (1989, 1994) equation, that relates the event frequency to the magnitude M_m of the main shock, the cutoff magnitude M_I and the time elapsed from the mainshock.

In this paper, I assume that the sequences can be approximated with Reasenberg and Jones equation, I apply the relation between energy and magnitude and I find analytically (see Section 2) an equation that describes the cumulative radiated energy as function of time. In the proposed law the aftershock radiated energy is expressed as a function of p and c parameters of the MOM, of the mainshock energy and of the energy radiated in a selected time period after the mainshock.

The description of seismic sequences in terms of energy or seismic moments has been already done in the other papers: Gentili and Bressan (2008) compared the radiated energy at short time after the mainshock with the one at the end of the sequence, Shcherbakov and Turcotte (2004) proposed a relation between the difference between the mainshock and the strongest aftershock magnitude and the sequence radiated energy, Kagan and Houston (2005) proposed a description of the sequence in terms of seismic moment, Zaliapin et al (2005) proposed a method for fitting cumulative moment.

An important feature of the approach proposed in this paper is that it allows to make an alternative evaluation of *p* and *c* parameters. Recently, the *c* parameter has been identified as related to the stress in the area, and is used for short term earthquake forecasting (EAST model - Shebalin et al., 2011). However, the value of *c* has been widely debated (Kagan and Houston, 2005, Lolli and Gasperini, 2006, Utsu et al., 1995, Shcherbakov et al., 2004, Kagan, 2004 and Lippiello et al., 2007). The origin of the debate is that the *c* term in the MOM is sensitive to the rate of seismicity for times close to the mainshock, i.e. when, due to the waveform superposition, it is more difficult to evaluate the seismicity rate, especially when small earthquakes are considered. The proposed approach overcomes this problem, because it is sensitive to strong magnitude earthquakes, i.e. the ones that are more easily detected.

A general law was proposed (see section 3) relating the energy radiated in a short time period after the mainshock and the difference in magnitude Δm between the mainshock and the strongest aftershock of the seismic sequence. The equations describing the radiated energy as function of time and the one on Δm were applied to 9 seismic sequences in California.

2. Temporal evolution of radiated seismic energy

The aftershock temporal decay previously described by Omori law (1894) was improved by Utsu (1961) in the MOM, that relates the rate ν of aftershocks with magnitude larger than M_1 to the time *t* elapsed after the main shock:

$$\nu(t, M_1) = \frac{K(M_1)}{(t+c)^p} \tag{1}$$

where $K(M_1)$ is related to the total number of earthquakes, c depends on the rate of activity in the earliest part of the sequence and *p* is related to the temporal decay of the aftershocks (Kisslinger and Jones, 1991). The Omori law was verified to have a good fit on hundreds of sequences (Utsu et al. 1995). Two examples of alternative description of seismicity rates are the modified stretched exponential (Gross and Kisslinger 1994) and the Band Limited Power Law (Narteau et al. 2003).

Both laws are characterized by an exponential decay for long times after the mainshock. Lolli and Gasperini (2006) and Gasperini and Lolli (2009) compared the quality of the fit of the three different laws on real data by using the corrected Akaike Information Criteria (AICc) and the Bayesian Information Criteria (BIC) and found that the exponential decay laws fit better the data if a large time span after the mainshock is considered, while for shorter time span (Lolli and Gasperini, 2006) the best fit is obtained by the MOM.

The energy distribution of the seismic sequence was described by the frequency-magnitude scaling of Gutenberg and Richter (1954) that states that:

$$Log_{10}(N(M_I)) = A - bM_I \tag{2}$$

where $N(M_I)$ is the number of earthquakes with magnitude larger than M_I, A is a measure of the regional level of seismicity (Kagan, 2004), while b depends on the proportion of large and small earthquakes (Gerstenberger et al, 2007).

It is debated if the Gutenberg and Richter (1954) law can be applied to the whole seismic sequence or only to the aftershocks (see Utsu 1969, Helmstetter and Sornette 2003).

Combining equations (1) and (2) Reasenberg and Jones (1989, 1994) proposed an aftershock occurrence model, which describes the rate of aftershocks with magnitude larger than M_I as a function of time and of the main shock magnitude:

$$\nu(t, M_I) = \frac{10^{a+b(M_m - M_I)}}{(t+c)^p} \tag{3}$$

where M_m is the magnitude of the main shock, c and p are the parameters of eq. (1), b is the parameter of equation (2) and a is the "productivity" (Gasperini and Lolli, 2006), related to the parameter A of equation (2) (Lolli and Gasperini, 2003):

$$a = A - bM_m - Log_{10}\left[\int \frac{1}{(t+c)^p}\,dt\right] \tag{4}$$

It was found that for some sequences equation (1) and therefore eq. (3) only approximately fits the data, because not only the mainshock, but also the aftershock can trigger a seismic sequence.

122 Abrupt increases of seismicity following the strongest aftershocks have been observed. This
123 behavior is described by the ETAS (Epidemic Type Aftershock Sequences) law (Kagan and
124 Knopoff 1981, Ogata 1988) that is a generalization of eq. (3).
125 The magnitude of an earthquake is related with its radiated energy by the regression (Gutenberg and
126 Richter, 1956):

127 $$\log_{10} E(M) = \alpha M + \beta \tag{5}$$

128 where α and β are constants and M is the magnitude. The parameters α and β depend on the
129 magnitude scale adopted.
130 In this paper I study the evolution of the radiated seismic energy assuming that, during the seismic
131 sequence, the magnitude or energy distribution is independent on time. This assumption is
132 consequence of the Reasenberg and Jones equation (3).
133 The energy of the aftershocks $E_{as}(t)$ of the sequence as function of time can be obtained by
134 integrating over the distribution of aftershocks magnitudes:

135 $$E_{as}(t) = \int_{M_c}^{M_m} E(m) \left(-\frac{dN(m,t)}{dm} \right) dm \tag{6}$$

136 where M_c is the completeness magnitude and N is the cumulative number of earthquakes with
137 magnitude greater than m at the time t, i.e.:

138 $$N(m,t) = \int_0^t \nu(\theta, m) d\theta \tag{7}$$

139 Substituting equation (3) into equation (7) and taking the derivative with respect to the magnitude
140 m, I obtain:

141 $$\frac{dN(m,t)}{dm} = -b \ln(10) 10^{a+b(M_m - m)} \int_0^t \frac{d\theta}{(\theta + c)^p} \tag{8}$$

142 Substitution of equations (8) and (5) into equation (6) gives:

143 $$E_{as}(t) = \Lambda(a, b, \alpha, \beta, M_m, M_c) \int_0^t \frac{d\theta}{(\theta + c)^p} \tag{9}$$

144 Where $\Lambda(a,b,\alpha,\beta,M_m,M_c)$ is:

145 $$\Lambda = \frac{b}{\alpha - b} 10^{\alpha M_c + \beta} \cdot \left[10^{a+\alpha(M_m - M_c)} - 10^{a+b(M_m - M_c)} \right] \quad (10)$$

146 The derivative of eq. (9) with respect to time is the equivalent of the Reasenberg and Jones model
147 for radiated energy rather than for number of earthquakes. Bressan et al. (2007) define the
148 parameter R_{ES} as the ratio between the energy radiated by the mainshock and the summation of the
149 energies radiated by all the aftershocks of a seismic sequence. Let

150 $$R_{ES}(t) = E_m / E_{as}(t) \quad (11)$$

151 where E_m is the radiated energy of the mainshock and $E_{as}(t)$ is the summation of the energies
152 radiated by till the time t after the mainshock. From equation (9):

153 $$Log(R_{ES}(t)) = Log(E_m) - Log(E_{as}(t)) = Log(E_m) - Log\left(\Lambda \int_0^t \frac{d\theta}{(\theta + c)^p} \right) \quad (12)$$

154 Let τ be a generic time smaller than t; from equation (12):

155 $$Log(R_{ES}(t)) = Log(R_{ES}(\tau)) - Log\left(1 + \frac{\int_\tau^t \frac{d\theta}{(\theta + c)^p}}{\int_0^\tau \frac{d\theta}{(\theta + c)^p}} \right) = Log(R_{ES}(\tau)) - f(t, c, p, \tau) \quad (13)$$

156 with:

157 $$f(t,c,p,\tau) = \begin{cases} Log\left[1 + \dfrac{(t+c)^{1-p} - (\tau+c)^{1-p}}{(\tau+c)^{1-p} - c^{1-p}} \right] & for\ p \neq 1 \\ Log\left[1 + \dfrac{\ln\left(\frac{t+c}{\tau+c} \right)}{\ln\left(\frac{\tau+c}{c} \right)} \right] & for\ p = 1 \end{cases} \quad (14)$$

158 Equation (13) states that the energy ratio evolution can be modeled using only the parameters c and
159 p of the Modified Omori Model, and the selected time intervals (0, t) and (0, τ). In addition, it states
160 that the ratio of amounts of energy radiated within two different time intervals and the ratio of
161 number of aftershocks within the same time intervals are equal. This result is important for both c

and p parameters evaluation. The Omori number-based approach treats all the events as having the same weight, also the smaller ones, which are partially lost immediately after the mainshock. The eq. (13) energy-based approach, vice-versa, gives a larger weight to larger earthquakes, that are the ones recorded in the catalogue. For this reason, the less reliable data affect more the number-based than the energy-based parameter estimation. Higher values of f mean that, after τ, a great amount of energy is radiated, decreasing the value of R_{ES}; f close to 0, vice-versa, means that almost all the energy of the sequence has been radiated within the time τ and that the contribution to the aftershock energy after the time τ is negligible. Figure 1 shows an example with the trend of f for c=0.1, τ=1 day and p=0.9, 1 and 1.1, respectively. For $t \to \infty$, finite values of τ and p>1, $f(t,c,p,\tau) \to Log\left[\frac{c^{1-p}}{c^{1-p}-(\tau+c)^{1-p}}\right]$ (see the asymptote of the curve for p=1.1). If $\tau \to t$, $f \to 0$; if $t < \tau$, $f < 0$.

<Insert Figure 1 here>

The equation (14) diverges for $t \to \infty$ if $p \leq 1$. This is a well-known problem related to the applicability of MOM (Utsu, 1961) and therefore Reasenberg and Jones (1989) equation for large time after the mainshock. Gasperini and Lolli (2009) for a set of Italian and Californian sequences with $5.2 \leq M_m \leq 7.1$ have shown that, for a time period of the order of 4 years, equations with an exponential decrease of the number of aftershock supply better results on real data than MOM. However, for shorter time after the mainshock (1 year), the power law distribution holds (Lolli and Gasperini, 2006). In this paper, I'll restrict the analysis to the domain of MOM applicability. In order to have an estimate of the distribution of the fluctuation of the energy respect to its mean value in time, I assumed that the ratio between energy and seismic moment is constant (e.g. Kanamori 1977: $E=M_0/2\text{x}10^4$ erg). This relation assumes that the stress drop is constant and has been debated in recent years. Recent papers (e.g. Malagnini et al. 2010, Gok et al 2009) show an increase of stress drop with seismic moment, therefore Kanamori equation should be seen as a

simplified relation. If the Kanamori 1977 relation is wrong, the previous equations can be rewritten in terms of seismic moment, where the term "energy" is substituted by "moment energy" defined as the seismic moment divided by $2x10^4$. For simplicity, in the following I will continue to refer it as seismic energy. Using Kanamori 1977 equation, the summation of radiated energy is equivalent to the summation of seismic moments. Zaliapin et al. (2005) showed that random fluctuations of the sum of seismic moments are very large, because it is the sum of power law distributed variables, i.e. heavy tailed random variables. A heavy tailed distribution is a distribution that assigns a non-ignorable probability to extremely large observations. The approximation of the fluctuation of the sum of seismic moments by a normal distribution is not justified (Zaliapin et al. 2005) and a large number of summands are needed to yield reliable results (Kagan and Houston, 2005).

Kagan and Houston (2005) propose an equation for the seismic moment rate in the hypothesis that p=1:

$$\dot{M} = \frac{k' \tau_{pk} \dot{M}_{pk}}{t + c'} \tag{15}$$

where c' is a coefficient similar to c but possibly with a different value, $\dot{M}_{pk}$ is the peak moment realize rate, τ_{pk} is the time the peak occurs and k' is a constant. Assuming that the ratio between energy and seismic moment is constant, equation (15) is compatible with (13) and (9) if c=c'.

Gentili and Bressan (2008), analyzing 8 seismic sequences in Northeastern Italy, found empirically a linear relation between the value of $\mathrm{Log}_{10}(R_{ES})$ at the end of the seismic sequence ($\mathrm{Log}_{10}[R_{ES}(T)]$) and its value at a time τ=24 hours after the mainshock ($\mathrm{Log}_{10}[R_{ES}(24)]$). The relation holds also for different time intervals after the mainshock; the time period of 24^h was chosen as a compromise between the stability of results (that needs large time intervals) and the need of an early estimate of R_{ES}. In particular, they found:

$$Log_{10}\left[R_{ES}(T)\right] = D \cdot Log_{10}(R_{ES}(24)) - B \tag{16}$$

With D=0.78, B=0.36, $\sigma(\mathrm{Log}_{10}[R_{ES}(T)])$=0.39 and R^2=0.81. The error on the parameters (unpublished result) was high: ΔD=±0.4 and ΔB=±1.1.

Comparing empirical equation (16) with analytical results of eq. (13), it can be seen that the parameter B it is not a constant, like in Gentili and Bressan paper, but it is a p and c dependent term. This caused the large uncertainty in B parameter estimation. A constant value of B could be possible if both p and c parameters were constant. The parameter p has been related with the surface heat flow (Mogi 1962, Kisslinger and Jones 1991, Marcellini 1995) or with the heterogeneity of the stress field (depending on the mainshock magnitude - Hainzl e Marsan 2008). The c parameter has been related to the magnitude of the static stress change after the mainshock (Dieterich 1994) or to the level of stress and seismogenic potential of the area (Shebalin et al 2011). A constant value of B can be hypotized if the studied sequences are close enough in space, time and mainshock magnitude that the parameters are unchanged.

The equation proposed in this paper is therefore a refinement of Gentili and Bressan (2008) equation. The parameter D estimated by Gentili and Bressan as equal to 0.8±0.4 is compatible with the value of 1 in eq. (13).

3. Strongest aftershock magnitude

Shcherbakov and Turcotte (2004) analyzed the partitioning of the released seismic energy between mainshock and aftershocks and its relation to Δm. They assumed that there is one only strongest aftershock in the seismic sequence and therefore the A and b parameters of the Gutenberg Richter equation are related one to the other:

$$A=bM^* \qquad (17)$$

where M^* is the magnitude of the strongest aftershock. With a method similar to the one used in this paper to obtain eq. (9), they found a relation between Δm and the ratio between the total energy radiated by the aftershocks $E_{as}(T)$, and the energy radiated by the mainshock E_m,:

$$\frac{E_{as}(T)}{E_m} = \frac{b}{\alpha - b} 10^{-\alpha \Delta m} \tag{18}$$

In particular, they obtained eq. (18) for α=3/2 in their paper. The equation was obtained considering the whole real seismic sequence ($m \leq M^*$, completeness magnitude = $-\infty$). If the completeness magnitude is taken into account, equation (18) becomes:

$$\frac{E_{as}(T)}{E_m} = \frac{b}{\alpha - b} 10^{-\alpha \Delta m} \left[1 - 10^{-(\alpha - b)(M^* - M_c)} \right] \tag{19}$$

That reduces to (18) for $\alpha > b$ and $M^* >> M_c$.

Gentili and Bressan (2008) rearranged the equation (18) in order to obtain a relation between of Δm and $R_{ES}(T)$:

$$\Delta m = -\frac{1}{\alpha} \log_{10} \left[\frac{E_{as}(T)}{E_m} \right] - \frac{1}{\alpha} \log_{10} \left(\frac{\alpha - b}{b} \right) = \frac{1}{\alpha} \log_{10} \left[R_{ES}(T) \right] + \frac{1}{\alpha} \log_{10} \left(\frac{b}{\alpha - b} \right) \tag{20}$$

The second addendum of the sum in equation (20) setting b~1 and α=3/2 (e.g. Utsu 2002) is approximately 0.2. From eq. (20) it is possible to see that Δm decreases with increasing E_{as}/E_m, for b-term fixed, and decreasing b, if E_{as}/E_m is fixed.

Substituting eq. (13) into eq. (20) we have:

$$\Delta m = \frac{1}{\alpha} \left[\log_{10}(R_{ES}(\tau)) + \log_{10} \left(\frac{b}{\alpha - b} \right) - f(T, c, p, \tau) \right] \tag{21}$$

4. Parameters dependence on the cutoff and mainshock magnitude

The value of c parameter obtained by fitting MOM is widely debated. Kagan and Houston (2005) proposed that c=0 or negative, and that the measured c>0 were due only to the underestimate of the rate of the number of earthquakes immediately after the mainshock. This could be coherent with the results of Lolli and Gasperini (2006) on 47 seismic sequences in Italy and California. They found that, increasing the minimum magnitude considered, c tends to 0. However, detailed studies on the seismicity after the mainshock (see e.g. Vidale et. al, 2003, Peng et al., 2007, Enescu et al., 2007) could exclude this hypothesis at least for some sequences, also because if a value different from 0

255 was wrongly assigned to c, for $t=c$ the percentage of lost event could be huge (e.g. 1/2 for $p=1$)
256 (Utsu et al., 1995).
257 Shcherbakov et al. (2004) found a relation between c and the minimum considered magnitude
258 (cutoff magnitude); a similar result was found by Kagan (2004) and Lippiello et al (2007).
259 All these papers agree on the fact that c evaluated from Omori law scales as:
260 $$c = c_0 10^{\varphi(M_m - M_1)} \quad (22)$$
261 where φ is of the order of 1 and c_0 is a constant or depends on the values of p and b of the sequence.
262 These results have been interpreted in different ways. Kagan claimed that the trend is an artifact due
263 to the superposition of the waveforms for events close to the mainshock (the Short Term Aftershock
264 Incompleteness hypothesis – Kagan, 2004). Gasperini and Lolli (2006) found a positive correlation
265 between p and c for sequence analyses in Italy and New Zealand and imputed it to the under
266 estimate of the number of earthquakes close to the mainshock. If, they say, c is overestimated due to
267 lost earthquakes, this could slow the Omori law decay in the first times after the mainshock; to
268 compensate this effect, the maximum likelihood test assigns a too high value of p.
269 On the other side, Nanjo et al. (2005, 2007) related it to a physical mechanism. In particular, in
270 Nanjo et al. (2005) the trend of c has been explained in terms of damage mechanics; according with
271 their paper, c is inversely proportional to the difference between the excess of stress induced by the
272 mainshock and the yield stress, i.e. the stress above which the medium has no more an elastic
273 behavior and there is a damage. Since it is reasonable that strongest aftershocks are connected with
274 regions with higher stress variation, c should be inversely proportional to the aftershock magnitude.
275 Lippiello et al (2007) evaluated the aftershock probability by a law that for long time after the
276 mainshock coincides with Omori law, but that for short times has a logarithmic behavior, in which c
277 depends on the cutoff magnitude. They applied the law to the fit of a dataset proposed by Peng et al.
278 2007, in which a careful high frequency filtering allowed the detection of a huge number of

aftershocks in Japan. The data appear to fit better this function than Omori law for short times after the mainshock.

Equation (22) has the important implication that for the same sequence, the choice of two different values of M_I, M_{I1} and M_{I2}, greatly affects the corresponding values c_1 and c_2 of c. Rearranging equation (22) I obtain:

$$\frac{c_1}{c_2} = 10^{\varphi(M_{I2}-M_{I1})} \tag{23}$$

This means, for example, that choosing M_{I2}=4 instead of M_{I1}=1 we would obtain a ~1000 times smaller value of c, if φ~1.

The function f of equation (13) depends on the parameters t, τ, c and p. While t and τ terms are input terms of the fit, if the terms c and/or p depend on the selected cutoff magnitude, this causes a dependence also of f function and therefore of the radiated energy evolution. This means that the trend of the observed radiated energy during time depends on the selected cutoff magnitude.

Differently from c, p was generally found to be independent on M_I (Utsu et al., 1995), which is equivalent to the fact that b-value of the Gutenberg and Richter law is constant throughout the aftershock activity (Utsu et al., 1995). On the other side, Ouillon and Sornette (2005) proposed a dependence of p on the mainshock magnitude M_m in their multifractal stress activation model. Their model is based on two hypotheses: rupture activation exponentially dependent by local stress and relaxation with long memory. They analyzed the California earthquake catalogue and stacked together sequences with mainshock within 0.5 magnitude units. They applied two different declustering approaches and found that p increases with magnitude by approximately 0.1-0.15 for each magnitude increase. The authors emphasize that this result can be obtained only by stacking together many sequences in order to average out the fluctuations. An analogous trend was found by Hainzl and Marsan (2008) applying many different declustering methods to the global earthquake catalog ISC. They explain this result in the framework of the rate and state friction model. The

303 values of p are occasionally significantly different between the two papers, probably due to the
304 different catalogue and the different time intervals for fitting the decays (Hainzl and Marsan, 2008).
305

306 ## *5. Application to California*

307 The proposed method has been applied to a set of 9 Californian seismic sequences in the years
308 1987-2003 with mainshock magnitude in the range [5.5, 7.3] (see Table 1).

309 <Insert Table 1 here>

310 The sequences were the same described in Shcherbakov and Turcotte (2004) with the exception of
311 24 November 1987 Superstition Hills one, for which the presence of two closely spaced strong
312 mainshocks, 12 hours one from the other, whose aftershocks are on different but close faults
313 (Magistrale et al. 1989), causes problems in cluster definition.
314 For most aftershocks of the analyzed sequences neither the seismic moment nor the energy is
315 determined, because they are too small. Therefore, I adopted the Southern California Seismic
316 Network catalog (http://www.data.scec.org/catalog_search/date_mag_loc.php) and the Northern
317 California Seismic Network catalog (http://www.ncedc.org/ncedc/catalog-search.html) and,
318 analogously to Kagan and Huston (2005) for smaller earthquakes, I assumed that the local
319 magnitude in these catalogues is always equivalent to moment magnitude. Assuming that the ratio
320 between seismic moment and energy is constant (or using "moment energy" instead of the real
321 radiated energy – see section 2), I calculated the energy from eq. (5) with α=3/2. The sequences
322 have been selected using a space-time window. Similarly to Shcherbakov and Turcotte 2004, a
323 circular space window has been chosen whose linear size L scales with the mainshock magnitude
324 M_m: L= $0.02 \times 10^{0.5 * Mm}$ (Kagan, 2002) and a time window has been selected of 2 years for M<7
325 mainshocks and of 3 years for larger Landers and Hector Mine earthquakes. The sequences were
326 considered concluded at the end of the selected time interval because the contribution of eventual
327 possible subsequent earthquakes was negligible respect to the overall aftershock energy. In addition,

328 an analysis on a too long time interval would exit from the domain of applicability of MOM
329 equation and an exponential decrease of the number of earthquakes should have been taken into
330 account (Lolli and Gasperini, 2006, Gasperini and Lolli, 2009). The completeness magnitude M_c
331 was obtained applying the EMR method (Woessner and Wiemer, 2005) by using Zmap (Wiemer,
332 2001) software (see Table 1). It is important to remark that EMR method applied to the whole
333 seismic sequence supplies an "overall sequence" completeness magnitude that does not take into
334 account the fact that the completeness changes with time. Helmstetter et al. (2006) e.g., found the
335 following relation for a set of California mainshocks:
336 $$M_c(M_m, t)=M_m - 4.5 - 0.75 \mathrm{Log}_{10}(t) \quad (24)$$
337 where t is the time (in days) after the mainshock. The change in completeness magnitude during
338 time, accordingly with Kagan (2004), causes the change of the values of c obtained from Omori law
339 fit.
340 In order to fit the data, a time τ chosen for the analysis was 1 day, accordingly with Gentili and
341 Bressan 2008.
342 Figure 2a-i shows the fit of the data using the new equation (eq. 13) proposed in this paper. For
343 comparison, the curve obtained by using the parameters of the MOM fitting has been added (dotted
344 lines).

345 <Insert Figure 2 here>

346 Thin continuous lines correspond to the real data; steps in the lines correspond to the large
347 aftershocks that cause a sudden increase of the cumulative energy radiated by the aftershocks, and
348 therefore a sudden decrease of $R_{ES}(t)$. Thick black lines correspond to the fit of the data. Deviations
349 from the fit are due both to physical and computational causes. From the physical point of view, the
350 inhomogeneity of the material in terms of rigidity, pre-existing fractures, stress distribution etc. can
351 cause a delayed or advanced fracture of single patches. Brittle or fractured material is characterized
352 by a smaller yield stress and fractures for smaller values of applied stress (e.g. Griffith, 1920); on

353 the other side, the stress itself is not homogeneous and some patches are characterized by higher
354 local stress. Das and Scholz (1981) proposed a model in which aftershock occur by static fatigue on
355 isolated locked fault patches, describing the evolution of earthquake nucleation in time as function
356 of both the medium characteristics and of the stress. From the computational point of view, the
357 assumptions of local magnitude equal to moment magnitude for all the earthquakes of the catalogue
358 and constant radiated energy/moment ratio (i.e. constant value of α) can cause over or under
359 estimates of the radiated energy. In addition, if the sum of seismic energy is considered equivalent
360 to the sum of seismic moments, large random fluctuations of this sum (see section 2) should be
361 considered.
362 The free parameters *c* and *p* are estimated using a maximum-likelihood estimate. One of the
363 problems in applying maximum likelihood method is defining the likelihood function to be
364 maximized. In particular, a model should be issued for the fluctuations of the independent variable.
365 The fluctuations of the cumulative energy are not normally distributed (see section 2). Zaliapin et al
366 (2005) propose the following pdf for the sum of seismic moments in the hypothesis that the
367 Gutenberg Richter parameter *b*~1:

368 $$g(x) = \frac{\sqrt{3}}{x\sqrt{\pi}} \exp\left(-\frac{16}{27x^2}\right) W_{\frac{1}{2},\frac{1}{6}}\left(\frac{32}{27x^2}\right) \qquad x > 0 \tag{25}$$

369 Where W is a Whittaker function (Abramowitz and Stegun, 1966), which can be calculated using
370 the confluent hypergeometric function U (Wolfram 1999):

371 $$W_{\frac{1}{2},\frac{1}{6}}(z) = \frac{z^{2/3} U\left(\frac{1}{6}, \frac{4}{3}, z\right)}{e^{z/2}}$$

372 In this paper, I assumed that the energy fluctuations pdf is the one of equation (25), that has a
373 maximum in *x*=1. The function to be maximized is therefore $Log(g(X))$ with $X = R_{ES} - f + 1$.

The analysis has been performed for magnitude greater than the completeness magnitude shown in Table 1. Table 2 shows the values of *c* and *p*, together with the values of R^2 and RMSE for the fit of the equation (13). I used a bootstrap method to calculate the uncertainties on *p* and *c* parameters. Bootstrap sample radiated energy catalogues are generated by drawing with replacement an equivalent amount of radiated energy from the original catalogue. For each of the bootstrap sample energy catalogues, *p* and *c* are calculated. The standard deviation of the distributions of *p* and *c* values is defined as the uncertainty on the parameters. It is important to remark that this approach does not take into account the fluctuations of R_{ES}(24). It will be the topic of a future paper.

<Insert Table 2 here>

The value of *c* is always greater than 0 in all except one case. Most sequences show high value of R^2 and small RMSE in the fit, confirming the good capability of eq. (13) in describing real data.

Figure 2j shows the values of *f* as a function of elapsed time from the mainshock at the completeness magnitude. While most sequences are characterized by *f* ranging between 0.1 and 0.4, in some cases *f* can reach larger values. Ridgecrest earthquake, e.g., shows a high value of *f* respect to the other sequences, due to the small value of *p* (see eq. (14)). Such high value causes a strong reduction of R_{ES} after the first day, i.e. a large relative productivity of aftershocks in terms both of number of events and of radiated energy (see Section 2).

5.1 Cutoff and mainshock magnitude dependence

In order to understand if *c* dependence on M_m-M_I is the one of equation (23), M_I has been varied between 1 and 5 for each sequence, with the constrain that at least 10 earthquakes were available for the fit; the *c* value corresponding to the completeness magnitude, c_{Mc}, has been added to the data. Setting $M_{I2}=M_c$ and $c_2= c_{Mc}$, equation (23) becomes:

$$\frac{c}{c_{M_c}} = 10^{\varphi(M_c - M_I)} \tag{26}$$

where c/c_{Mc} depends on the completeness magnitude of the analyzed sequence and on the cutoff magnitude adopted, while it does not depend neither on c_0 nor on M_m. This allows to make a comparison also among different sequences. Figure 3a shows the values of c/c_{Mc} as a function of the difference between completeness the cutoff magnitude[1]. Different symbols correspond to different sequences.

<Insert Figure 3 here>

It is possible to see that choosing M_I within one magnitude unit from the completeness magnitude ($M_c - M_I \in [-1, 1]$) the ratio c/c_{Mc} remains stable, close to 1. This result shows the robustness of the method, because the value of c remains stable also *below* the completeness magnitude. Therefore, possible fluctuations in completeness magnitude estimate due to different estimation method applied, do not affect the results. This is due to the low contribution of smaller earthquakes to the whole radiated energy. On the other side, increasing the cutoff magnitude ($M_I > M_c+1$ i.e. $M_c - M_I < -1$), c increases, or decreases, or remains stable, depending on the sequence and does not have a defined trend; in particular, c ranges from 0 to 2.6 times the c_{Mc} at the completeness magnitude.

In order to understand a possible cause of the variability of c for $M_c - M_I < -1$, Fig. 3b shows c as a function of the number N of earthquakes considered for the fit. The N earthquakes used in the test are not chosen randomly, but are the ones corresponding to each cutoff magnitude of Fig. 3a. In this way, the smaller number of earthquakes is partially compensated by the fact that they are the larger, and therefore the more relevant for energy evaluation. The values of c are stable for $N \geq 100$ earthquakes ($c/c_{Mc} \in [0.93, 1.15]$), while for smaller number of earthquakes the fluctuations are larger. In Fig. 3a the sequence symbols are marked in black if $N \geq 100$. I assume that c variability of Fig. 3a is not a physical effect, but it is due to large fluctuations in cumulative energy estimation previously described and to approximations due to the use of eq. (5). The values of c should be therefore independent on M_I and constant. In all except one case, the inferred c value is greater than

[1] This approach cannot be applied for Baja California sequence for which $c_{Mc}=0$. However, since changing M_I, the value of c remains unchanged, for simplicity the ratio has been substituted by 1.

421 0, which confirms Utsu's thesis that at least in some cases, *c* value cannot be assumed always equal
422 to 0.
423 In order to compare the previous results with classical parameter estimation methods, Figure 3c
424 shows the value of *c* and *p* on the same sequences using the maximum likelihood procedure applied
425 to the modified Omori formula as proposed by Ogata (1983) and implemented in Zmap software.
426 The dispersion of *c* parameter is larger, ranging from 10^{-3} to 10^{2} times the value of c_{Mc}. Selecting
427 only the cases in which $M_I \geq M_c$ and $N \geq 100$ (black symbols in Fig. 3c) a trend compatible with eq.
428 (23) was found. In particular $\varphi=0.7$. Figure 3d shows the normalized function $c/[c_{Mc}10^{0.7(Mc-MI)}]$,
429 with the constrain $M_I \geq M_c$, as function of *N*. It can be seen that the MOM fit is extremely sensitive to
430 the number of considered earthquakes, and if a small number of earthquakes is considered, the
431 inferred values of the function range from 10^{-1} to 10^{3} times the values of the theoretical curve.
432 Figure 3c shows that the method is sensitive also to the completeness magnitude, because below
433 M_c-M_I=0 the data does not follow the straight line $c / c_{M_c} = 10^{0.7(M_c - M_I)}$.
434 Accordingly with Kagan (2004) the dependence of *c* on M_I parameter is an artifact in Omori law
435 fitting, due to the loose of data for times close to the mainshock (see eq. 24). The fact that a
436 different approach to *c* value estimation finds constant values of *c* supports Kagan's thesis.
437 Figure 4a and b show the normalized value of *p* as a function of M_c-M_I and of *N*, respectively,
438 applying the method proposed in this paper.
439 <Insert Figure 4 here>
440 Also in this case, no relation was found between the parameter and M_c-M_I. An instability of the
441 results was detected for $N<100$. In this case, however, the result is much more stable; *p* ranges from
442 0.8 to 1.2 times the value of *p* at the completeness magnitude (p_{Mc}), while if only the cases $N \geq 100$ is
443 considered, it ranges between 0.99 and 1.04 p_{Mc}. Figure 4c and d show the normalized value of *p* as
444 a function of M_c-M_I and of *N*, respectively, applying the modified Omori formula as proposed by
445 Ogata (1983) and implemented in Zmap software. It can be seen that the range of variation of *p* is

larger than in the energy-based evaluation, ranging from 0.6 to 3.2 times the value at the completeness magnitude if all values of N and M_I are considered, that reduces to [0.9-1.8] p_{Mc} if only $M_I \geq M_c$ and $N>100$ is considered. The approach proposed in this paper for p value estimation is therefore more stable. It is important to remark that while the method is more stable for a single sequence, it is however dependent also on the fluctuations of the energy of the strongest earthquakes before τ, that affect $R_{ES}(\tau)$, especially if τ is small; it is therefore not necessary more stable for multiple repeats of the same sequence. This problem could be solved by a smoothing of the data and will be topic of a future paper.

In order to investigate the stability of the parameters using energy based approach for different values of τ, Figure 5 shows the comparison among the values of c/c_{Mc} and p/p_{Mc} for τ equal to 12, 24 and 48 hours, as function of N.

<Insert Figure 5 here>

From the figure it can be seen that the parameters remain stable in all the cases for $N \geq 100$, while for $N<100$ larger values of τ supply more stable results. The quality of the fit generally decreases, with decreasing of the time τ. For τ equal 1 hour, for example, the quality of the fit is so poor that R^2 is close to 0 for most sequences. This is probably related to fact that the cumulative energy is less smoothed when a smaller number of events is involved. Abrupt changes of radiated energy, corresponding to larger aftershocks immediately after the mainshock, cause large fluctuations of $R_{ES}(\tau)$ if τ is small. In order to state that the variables $\log_{10}(c/c_{Mc})$ calculated with energy-based approach (Fig. 3a) and M_c-M_I are uncorrelated, I computed the linear correlation coefficient R and estimated its statistical significance (see e.g. Davis, 1986). I used only the data with $N \geq 100$ and $c_{Mc} \neq 0$. The null hypothesis H_0 is that $R=0$, the alternative is that $R \neq 0$. I compared the two hypotheses by using the Student-t statistics:

$$t = \sqrt{\frac{R^2(n-2)}{1-R^2}} \tag{27}$$

Where n is the number of samples. If t is greater than a threshold (available on statistical tables), corresponding to a significance level of 0.05 for degrees of freedom n-2, the existence of correlation can be asserted at a significance level of 0.05; conversely, for smaller values of t, the hypothesis H_0 cannot be rejected, and the two variables are uncorrelated at a significance level of 0.05. Table 3 shows the values of R and t for the two variables.

<Insert Table 3 here>

From Student-t test the two variables result uncorrelated. Since eq. (26) fails in describing the real data, when the influence of artifacts due to the loss of small magnitude aftershocks is reduced, this implies a failure also of equations (22) and (23), of which eq. (26) is a consequence.

Table 3 shows the correlation coefficient R and the value of t for p/p_{Mc} vs. M_c-M_I too. From Student-t test the two variables appear uncorrelated.

The independence of c and p on M_I implies that also f is independent. Figure 2*j* should be regarded as the real value of f, regardless of the cutoff magnitude applied. R_{ES} depends on both $R_{ES}(\tau)$ and f. $R_{ES}(\tau)$ increases with increasing cutoff magnitude M_I, because E_m remains unchanged, while E_{as} decreases, if smaller earthquakes are eliminated. The trend of $\mathrm{Log}(R_{ES}(t))$ is however independent on M_I, except for a shift, which depends on $\mathrm{Log}(R_{ES}(\tau))$ value. This result is unsurprising, since for the Gutenberg Richter equation the trend of radiated energy should be independent (except for a shift) on the selected cutoff magnitude.

In order to analyze the p parameter dependence on M_m, I divided the classes of seismicity at steps of 0.5 magnitude units and I calculated the mean and the standard deviation of the value of p inferred with the method proposed in this paper. Figure 6 shows the results together with their fit. For comparison, the fit for one declustering technique of Ouillon and Sornette (2005) and one of Hainzl and Marsan (2008) data has been added.

<Insert Figure 6 here>

494 Accordingly with this paper data, *p* increases with magnitude by 0.20 for each magnitude increase,
495 and the value of R^2 is 0.73.The results can be compared only qualitatively, due to the poor statistics
496 of this paper results for M>6. The analysis by using the Student-t statistics confirms a positive
497 correlation of the two variables with a significance level of 0.05 (see Table 3). A direct analysis
498 using the *p* values of all the sequences, without supplying a mean value, gives a positive correlation
499 only increasing the significance level to 0.15.This confirms, in the limits of the small statistics used,
500 the assertion of Ouillon and Sornette (2005) that the correlation can be found considering together
501 several sequences, while it is generally not true for the single sequence.
502 The *c* parameter shows a not relevant dependence on M_m, with a large scatter of the parameter (see
503 Table 3).
504 A last test has been done to verify if the positive correlation between *p* and *c* parameters found by
505 Gasperini and Lolli (2006) for Italy and New Zealand could be found also applying energy based
506 method. The values of *R* and *t* are shown in Table 3. The two variables are not correlated, because
507 of the different method adopted in their estimation. This supports Gasperini and Lolli (2006) thesis
508 that the correlation was due to the wrong estimate of *c*.

509 **5.2 Strongest aftershock magnitude estimation**

510 Table 4 shows the values of the 3 terms of equation (21) for the analyzed sequences for $M_I=M_c$. For
511 comparison, also the value of $\mathrm{Log}_{10}[R_{ES}(T)]$ at the end of the sequence has been added in the last
512 column. The *b*-dependent term has been calculated setting α=3/2 (Gutenberg and Richter, 1956) and
513 using *b* values listed Shcherbakov and Turcotte (2004), with the exception of San Simeon value
514 (b=1.17±0.09), that was calculated manually using Zmap software, because in Shcherbakov and
515 Turcotte (2004) paper only 100 days of the sequence were available. The last rows show the mean
516 and the standard deviation of each column. The 6th column shows the value of Δm (theoretical)
517 deduced applying equation (21).

518 <Insert Table 4 here>

519 The mean theoretical and the real value of Δm are similar and close to the value of 1.2 of the Båth
520 law and the standard deviation is 0.4. The mean of the difference between the true value of Δm and
521 the theoretical one (obtained from eq. 21) is 0.1 and its standard deviation is 0.1, compatible with a
522 magnitude assessment accuracy of 0.1. The mean value of f and its standard deviation, 0.37±0.37, is
523 similar to the result found by Gentili and Bressan (2008) (B=0.36±1.1), with a smaller standard
524 deviation.

525 <Insert Figure 7 here>

526 The reason why Gentili and Bressan (2008) found a good correlation between $\mathrm{Log}_{10}[R_{ES}(T)]$ and
527 $\mathrm{Log}_{10}[R_{ES}(24)]$, even if the c and p parameters changed from one sequence to the other, is that f is
528 generally lower than $\mathrm{Log}_{10}[R_{ES}(24)]$ (see Table 4), or, in other words, that most of the sequence
529 energy is radiated in the first 24 hours. Making the same fit of Gentili and Bressan (2008) on
530 Californian data (see Fig. 7) I found D=1.0±0.4 and B=-0.2±0.7, compatible with both Gentili and
531 Bressan result and the value of f found in this paper. Even if the value of R^2 is high, Whittier
532 Narrows and Ridgecrest sequences (shown by an arrow in Fig. 7), have values of $R_{ES}(T)$
533 anomalously low respect to the best fit line. This anomaly is due to the high value of f that in these
534 cases reaches the 50% and the 70% of the value of $\mathrm{Log}_{10}[R_{ES}(24)]$, respectively (see Table 4). This
535 is due to two different reasons: Whittier Narrows is characterized by a high value of c; this means
536 that the onset of the power low decay is later than in other sequences and therefore there is a high
537 frequency of earthquakes (high radiated energy) also after the first day. Ridgecrest, vice-versa, is
538 characterized by a very low value of p. This means that the frequency of the earthquakes (radiated
539 energy) decreases slowly and therefore it is still high after the first day.

540 <Insert Figure 8 here>

541 Figure 8*a*-*c* shows the ratio between of each term of eq. (21) and their sum. Note that, since f is
542 positive (see Fig 3*j*), the term $-f$ is negative and therefore the ratio can be greater than 1 and smaller
543 than -1. Figure 8a shows the ratio for the $R_{ES}(24)$ dependent term. The ratio is generally close to 1

544 (mean 1.18, standard deviation 0.51) except in the cases of the abovementioned sequences 1 and 6
545 (Whittier Narrows and Ridgecrest), corresponding to high negative values of -*f* term (see Fig. 8b);
546 the -*f* term has a generally smaller ratio (mean -0.37, standard deviation 0.54); the *b*-dependent term
547 (see Fig. 8c) has less variable ratio (mean 0.19, standard deviation 0.12).
548 Figure 8d shows, for each sequence, the absolute value of the 3 terms of eq. (21) divided by the sum
549 Σ of their absolute values. From the figure, it is possible to see that the energy dependent term
550 absolute value is preponderant being always greater than 50% with mean approximately the 70%;
551 this is true both for the sequences in which the strongest aftershock is within the first 24^h, and for
552 the ones (Whittier Narrows, Ridgecrest and Baja California) for which the strongest aftershock
553 occurs later. The *b* and *f* dependent terms have similar contributions, with high variability from one
554 sequence to the other, with a slightly larger contribution of *f*. In Table 4, it is interesting to notice
555 also the differences between Ridgecrest and Hector Mine sequences. The two sequences have
556 similar values of both the energy and the *b* dependent terms (see Table 4). The differences of Δm
557 are due to the *f* term. The huge value of *f* (Table 4, 7^{th} raw) of the Ridgecrest sequence respect to the
558 other is due to a small value of *p* (Table 2 row 7 and discussion in section 2). It is therefore a
559 difference in *p* and not in *b* that drives a large difference in Δm.

560 ## *6. Conclusions*

561 In this paper, a new temporal description of seismic sequences in terms of $R_{ES}(t)$ ratio has been
562 shown. In particular, the analytical description of $R_{ES}(t)$ as function of $R_{ES}(\tau)$ with $\tau<t$ and of
563 $f(t,c,p,\tau)$ (equation 13) has been proposed.
564 In the following, the main results obtained in this paper are listed and described.

565 1. ***Real data description.*** The equation (13) has been applied to 9 seismic sequences in
566 California. Real data are characterized by sudden steps in $R_{ES}(t)$, which cause deviations
567 from the fit line and are due both to physical and to computational causes (see section 5).

However, most sequences show high value of R^2 and small RMSE in the fit, confirming the good capability of eq. (13) in describing real data.

2. ***Comparison with relations in literature.*** The data are generally compatible with an empirical relation proposed by Gentili and Bressan (2008) relating $R_{ES}(T)$ and $R_{ES}(\tau)$ where T is the time of the end of the sequence and $\tau = 24^h$. However, the proposed equation (13) should be considered an improvement in radiated energy trend description, because a constant term in Gentili and Bressan (2008) equation is replaced by a p and c dependent one, that explains deviations from the fit of Gentili and Bressan (2008) equation (see Fig. 7). In addition, eq. (13) is compatible with Kagan and Houston (2005) equation for seismic moment rate (eq. (16) in this paper) if $c=c'$.

3. ***Parameter estimation: c.*** The description of f in terms of c and p allows to perform an estimate of the two parameters that is alternative to the MOM fitting. The problem of c estimation arises from the fact that the frequency of earthquakes in the MOM depends on c only for short times after the mainshock, when it is more difficult detecting the earthquakes; therefore the inferred c is often interpreted, at least partially, as an artifact (Kagan, 2004, Lolli and Gasperini, 2006, Utsu et al 1995), due to the fitting of incomplete data for times close to the mainshock. Equation (13) of this paper allows to circumvent the problems connected with MOM fitting, because this approach is less sensitive to variation in completeness magnitude (strongest earthquakes influence more the overall radiated energy than the smaller ones) and f is sensitive to the value of c for longer times. The values of c obtained by applying equation (13) to 9 Californian sequences, show no dependence on the cutoff magnitude M_I, confirming the Kagan (2004) thesis that the dependence of c on M_I ($c = c_0 10^{\varphi(M_m - M_I)}$) is an artifact. On the other side, in all except one case, the inferred c value is greater than 0, in accordance with Utsu et al. (1995). If these results will be confirmed on a larger database, they will invalidate the Nanjo et al. (2005) thesis that the c

parameter varies in space and is proportional to the local difference between yield stress and excess stress induced by the mainshock. The obtained values of $c \geq 0$ are compatible with both the Dieterich (2004) physical model, that predicts an initially constant aftershock rate before the rate begins to decay as a power law with time, and with Shebalin (2011) model, that inversely relates the *c* value and the seismogenic potential of the area.

4. ***Parameters estimation: p.*** An increase of p with M_m have been found by binning the magnitude M_m axis and evaluating the mean of p; in particular, a positive correlation has been observed at a significance level of 0.05. This is compatible both with Ouillon and Sornette (2005) multifractal activation model and with Hainzl and Marsan (2008) treatment, based on rate and state model. No correlation was found between p and c parameters. This is unsurprising, because accordingly with Gasperini and Lolli (2006) it was an artifact, due to the wrong fitting of the c parameter of using MOM.
5. ***New relation for Δm.*** A new equation (eq. 21) has been proposed, that describes the difference Δm between the mainshock and the strongest aftershock earthquake energy as function the sum of three terms: one depending on $R_{ES}(\tau)$, one on the b parameter of the Gutenberg Richter equation and one on $f(\tau)$. The mean estimated values of Δm using equation (21) and the real one are similar and close to the value of 1.2 of the Båth law. An analysis has been performed to understand which term of equation (21) is the more relevant for the value of Δm if τ=1 day. It emerges that the contribution of the energy dependent term is preponderant, being always greater than 50% of the sum of the tree terms absolute values, with mean approximately the 70%; this is true both for the sequences in which the strongest aftershock is within the first 24^h, and for the ones (Whittier Narrows, Ridgecrest and Baja California) for which the strongest aftershock is after.

Acknowledgments

I would like to thank Gianni Bressan and Riccardo Giannitrapani for their valuable discussions and suggestions. I also wish to acknowledge the two unknown reviewers for their helpful comments.

References

Abramowitz, M., Stegun, I. A., 1966. Handbook of Mathematical Functions (National Bureau of Standards Applied Mathematics Series 55). National Bureau of Standards, Washington, D.C..

Båth, M., 1965. Lateral inhomogeneities in the upper mantle. Tectonophysics, 2: 483-514.

Bressan, G., Kravanja, S., Franceschina, G, 2007. Source parameters and stress release of seismic sequences occurred in the Friuli-Venezia Giulia region (Northeastern Italy) and in Western Slovenia. Phys. Earth Planet. Inter., 160: 192-214.

Davis, J.C., 1986. Statistics and Data Analysis in Geology, John Wiley & Sons, New York.

Das, S., Scholz, C. H. , 1981. Theory of Time-Dependent Rupture in the Earth. J Geophys. Res., 86: 6039-6051.

Dieterich, J., 1994. A constitutive law for rate of earthquake production and its application to earthquake clustering. J. Geophys. Res. 99:2601-2618 .

Enescu, B., Mori, J., Miyazawa, M., 2007. Quantifying early aftershock activity of the 2004 mid-Niigata Prefecture earthquake (Mw6.6). J. Geophys. Res., 112: B04310, doi:10.1029/2006JB004629.

Gasperini, P., Lolli, B, 2006. Correlation between the parameters of the aftershock rate equation: Implications for the forecasting of future sequences. Phys. Earth Planet. Inter., 156: 41-58.

Gasperini, P., Lolli, B., 2009. An empirical comparison among aftershock decay models. Phys. Earth Planet. Inter., 175: 183-193.

640 Gentili, S., Bressan, G., 2008. The partitioning of radiated energy and the largest aftershock of
641 seismic sequences occurred in the northeastern Italy and western Slovenia. J Seism., 12: 343–354.
642 Gerstenberger, M.C., Jones, L. M., Wiemer, S. , 2007. Short-term Aftershock Probabilities: Case
643 Studies in California. Seismological Research Letters, 78(1): 66-77.
644 Gok, R., Hutchings, L., Mayeda, K, Kalafat, D., 2009. Source Parameters for 1999 North Anatolian
645 Fault Zone Aftershocks. Pure appl. Geophys., 166: 547-566.
646 Griffith, A., A., 1920. The phenomena of rupture and flow in solids, Phil. Trans. R. Soc. London
647 Ser. A, 221:169-198.
648 Gross, S.J., Kisslinger, C., 1994. Tests of models of aftershock rate decay. Bull. Seism. Soc. Am.,
649 84: 1571-1579.
650 Gutenberg, B., Richter, C.F., 1954. Seismicity of the Earth and Associated Phenomena. Princeton
651 University Press, Princeton, N.J., pp. 17-19.
652 Gutenberg, B., Richter, C.F., 1956. Earthquake magnitude, intensity, energy and acceleration. Bull.
653 Seism. Soc. Am., 46: 105-145.
654 Hainzl, S., Marsan, D., 2008. Dependence of the Omori-Utsu law parameters on the main shock
655 magnitude: Observations and modeling. J. Geophys. Res., 133: B10309, doi:
656 10.1029/2007JB005492.
657 Helmstetter, A., Sornette, D., , 2003. Båth's law derived from the Gutenberg-Richter law and from
658 aftershock properties. Geophys. Res. Lett., 30(20): 2069, doi:10.1029/2003GL018186.
659 Helmstetter, A., Kagan, Y.Y., and Jackson, D.D., 2006. Comparison of short-term and time-
660 independent earthquake forecast models for southern California. Bull. Seism. Soc. Am., 96, 90-106.
661 Kagan, Y.Y., 2002. Aftershock Zone Scaling. Bull. Seism. Soc. Am. 92: 641-655.
662 Kagan, Y.Y., 2004. Short-Term properties of earthquake catalogs and models of earthquake source.
663 Bull. Seism. Soc. Am., 94: 1207-1228.
664 Kagan, Y.Y., and Houston, H., 2005. Relation between mainshock rupture process and Omori's law
665 for aftershock moment release rate. Geophys. J. Int. , 163: 1039-1048.

666 Kagan, Y.Y., Knopoff, L., 1981. Stochastic synthesis of earthquake catalogs. J. Geophys. Res., 86:
667 2853-2862.
668 Kanamori, H., 1977. The energy release of great earthquakes, J. Geophys. Res. 82: 2981-2987.
669 Kisslinger, C., Jones, L.M., 1991. Properties of aftershocks in southern California. J. Geophys.
670 Res., 96: 11,947-11,958.
671 Lippiello, E., Bottiglieri, M., Godano, C., de Arcangelis, L., 2007. Dynamical scaling and
672 generalized Omori law. Geophysical Research Letters, 34: doi:10.1029/2007GL030963.
673 Lolli, B., Gasperini, P., 2006. Comparing different models of aftershock rate decay: The role of
674 catalog incompleteness in the first times after main shock. Tectonophysics 423: 43-59.
675 Magistrale, H., Jones, L., Kanamori, H., 1989. The Superstition Hills, California, earthquakes of 24
676 November 1987. Bull. Seism. Soc. Am., 79: 239-251.
677 Malagnini, L., Nielsen, S., Mayeda, K., Boschi, E., 2010. Energy radiation from intermediate- to
678 large-magnitude earthquakes: Implications for dynamic fault weakening. J. Geophys. Res., 115:
679 B06319, doi:10.1029/2009JB006786.
680 Marcellini, A., 1995. Arrhenius behaviour of aftershock sequences. J. Geophys. Res. 100: 6463-
681 6468.
682 Mogi, K. 1962. On the time distribution of aftershocks accompanying the recent major earthquakes
683 in and near Japan. Bull. Earthq. Res. Inst.,Univ. Tokyo, 40:175-185.
684 Nanjo, K.Z., Enescu, B., Shcherbakov, R., Turcotte, D. L., Iwata, T., Ogata Y., 2007. Decay of
685 aftershock activity for Japanese earthquakes. J. Geophys. Res., 112: B08309,
686 doi:10.1029/2006JB004754.
687 Nanjo, K.Z., Turcotte, D.L., Shcherbakov, R., 2005. A model of damage mechanics for the
688 deformation of the continental crust. J. Geophys. Res., 110: B07403, doi:10.1029/2004JB003438.
689 Narteau, C., Shebalin, P., Hainzl, S., Zöller, G., Holschneider, M., 2003. Emergence of a band-
690 limited power law in the aftershock decay rate of a slider-block model. Geophysical Research
691 Letters, 30(11): 1568, Doi:10.1029/2003gl017110.

692 Ogata, Y., 1983. Estimation of the parameters in the modified Omori formula for aftershock
693 frequencies by the maximum likelihood procedure. J. Phys. Earth, 31:115-124.
694 Ogata, Y., 1988. Statistical models for earthquake occurrence and residual analysis for point
695 processes. J. Am. Stat. Assoc., 83: 9-27.
696 Omori, F., 1894. On the aftershocks of earthquakes. Journal of the College of Science, Imperial
697 University of Tokyo, 7: 111-200.
698 Ouillon, G., Sornette, D. , 2005. Magnitude-dependent Omori law: Theory and empirical study. J.
699 Geophys. Res.110: B04306, doi:10.1029/2004JB003311.
700 Peng, Z., Vidale, J.E., Ishii, M., Helmstetter, A., 2007. Seismicity rate immediately before and after
701 main shock rupture from high-frequency waveforms in Japan. J. Geophys. Res., 112: B03306
702 doi:10.1029/2006JB004386.
703 Reasenberg, P.A., Jones, L.M., 1989. Earthquake hazard after the mainshock in California. Science,
704 243: 1173-1176.
705 Reasenberg, P.A., Jones, L.M., 1994. Earthquake aftershocks: update. Science, 265: 1251-1252.
706 Richter, C.F., 1958. Elementary Seismology. Freeman, San Francisco, California, 768 pp.
707 Scholz, C.H., 1990. The Mechanics of Earthquakes and Faulting. Cambrige University Press.
708 Shcherbakov, R., Turcotte, D. L. , 2004. A modified form of Båth's law. Bull. Seism. Soc. Am.,
709 94(5): 1968-1975.
710 Shcherbakov, R., Turcotte, D.L., Rundle, J.B., 2004. A generalized Omori's law for earthquake
711 aftershock decay. Geophys. Res. Lett., 31: L11613.
712 Shebalin, P., Narteau, C., Holschneider, M., Schorlemmer, D., 2011. Short-Term Earthquake
713 Forecasting Using Early Aftershock Statistics. Bull. Seism. Soc. Am. , 101: 297-312.
714 Utsu, T., 1957. Magnitude of earthquakes and occurrence of their aftershocks. J. Seism. Soc. Jap.,
715 10: 35-45.
716 Utsu, T., 1961. A statistical study of the occurrence of aftershocks. Geophys Mag., 30: 521-605.

717 Utsu, T., 1969. Aftershocks and earthquake statistics (I) - Some parameters which characterize an
718 aftershock sequence and their interrelations. J. Fac. Sci. Hokkaido Univ, Ser.VII, 3: 121-195.
719 Utsu, T., 2002. Relationship between magnitude scales. In: H.K. W. H. K. Lee, P. C. Jennings, and
720 C. Kisslinger (Editor), International Handbook of Earthquake and Engineering Seismology.
721 Academic Press, Amsterdam, pp. 733–746.
722 Utsu, T., Ogata, Y., Matsu'ura, R.S., 1995. The centenary of the Omori formula for a decay law of
723 aftershock activity. Journal of Physics of the Earth, 43: 1-33.
724 Vidale, J.E., Cochran, E.S., Kanamori, H., Clayton R.W., 2003. After the lightning and before the
725 thunder; non-Omori behavior of early aftershocks?, AGU Fall Meeting. Eos Trans. AGU Fall Meet.
726 Suppl., San Francisco, California, 8–12 December 2003.
727 Wiemer, S., 2001. A software package to analyze seismicity: ZMAP. Seism. Res. Lett., 72: 373-
728 382.
729 Wolfram, S., (1999) The Mathematica Book, 4th ed. Cambridge University Press.
730 Woessner, J., Wiemer, S., 2005. Assessing the quality of earthquake catalogues: Estimating the
731 magnitude of completeness and its uncertainty. Bull. Seism. Soc. Am., 95: 684-698.
732 Zaliapin, I. V., Kagan, Y. Y., Schoenberg, F. P., 2005. Approximating the Distribution of Pareto
733 Sums. Pure appl. Geophys., 162: 1187-1228.

Figure captions

Figure 1: The trend of f for c=0.1, τ=1 day and p=1.1, p=0.9, p=1. The asymptote for p=1.1 is also shown.

Figure 2: (a-i) $R_{ES}(t)$ vs. time (in days) for 9 Californian seismic sequences: (a) Whittier Narrows, (b) Upland (c) Sierra Madre (d) Landers (e) Northridge (f) Ridgecrest (g) Hector Mine (h) Baja California (g) San Simeon. Thin line: real data. Thick line: maximum likelihood fit. Dotted line: Parameters from MOM fit. (j) f as a function of time for the seismic sequences.

Figure 3: (a) c/c_{Mc}, calculated by using the energy based approach, as a function of M_c-M_I; the symbols marked in black correspond to $N\geq100$. (b) c/c_{Mc}, calculated by using the energy based approach, as a function of the number N of earthquakes. (c) c/c_{Mc}, calculated by using Omori law, as a function of M_c-M_I; the symbols marked in black correspond to $N\geq100$ and $M_I\geq M_c$. (d) $c/[c_{Mc}10^{0.7(Mc-MI)}]$ calculated by using Omori law, with the constrain $M_I\geq M_c$, as a function of the number of earthquakes.

Figure 4: (a) p/p_{Mc}, calculated by using the energy based approach, as a function of M_c-M_I; the symbols marked in black correspond to $N\geq100$. (b) p/p_{Mc}, calculated by using the energy based approach, as a function of the number of earthquakes. (c) p/p_{Mc}, calculated by using Omori law, as a function of M_c-M_I; the symbols marked in black correspond to $N\geq100$ and $M_I\geq M_c$. (d) p/p_{Mc}, calculated by using Omori law, with the constrain $M_I\geq M_c$, as a function of the number of earthquakes.

Figure 5: c/c_{Mc} as function of N using different values of τ. Circles: τ=1 day. Squares: τ=0.5 days. Diamonds: τ=2 days.

759

760 **Figure 6:** Mean of p as function of M_m. Thick dashed line corresponds to the minimum squares fit
761 of the data. Two of the fitting line proposed by Ouillon and Sornette (2005) (O&S – dotted line) and
762 Hainzl and Marsan (2008) (H&M – dot-dashed line) are shown.

763

764 **Figure 7:** $\mathrm{Log}_{10}[R_{ES}(T)]$ vs. $\mathrm{Log}_{10}[R_{ES}(24)]$ for the 9 sequence analyzed. Sequences with
765 $\mathrm{Log}_{10}[R_{ES}(T)]$ far from the fit line are shown with an arrow.

766

767 **Figure 8:** (a-c) Ratio between of each term of eq. (21) and their sum. (d) Absolute value of the 3
768 terms of eq. (21) divided by the sum of their absolute values. Each number corresponds to a
769 different sequence as listed in Table 1.

Table captions

Table 1: Main characteristics of the analyzed sequences. *N*: sequence number; *Main date*: mainshock date (UTC). *Lat* and *Lon*: north latitude and east longitude of the main shock (degrees); M_m: mainshock local magnitude; M_c: sequence completeness magnitude; M_a: strongest aftershock local magnitude; *Aft date*: strongest aftershock date (UTC).

Table 2: Parameters of the analyzed sequences. *N*: sequence number; *p* and *c*: *p* and *c* parameters of the Modified Omori Law; RMSE: Root Mean Square Error of the fit; R^2: coefficient of determination.

Table 3: Correlation analysis between different parameters. *R*: correlation coefficient; *t*: value of t-Student statistics for the null hypothesis of no correlation. *p*, M_m (3 points): correlation obtained between *p* mediated over all sequences with mainshock magnitude M_m inside 0.5 magnitude bin and M_m; (9 points): correlation between *p* and M_m.

Table 4: Equations (13) and (21) parameters. *N*: sequence number; Theoretical Δm: difference between mainshock and strongest aftershock magnitude obtained applying evaluated parameters to equation (21). Real Δm: real difference.

Figures

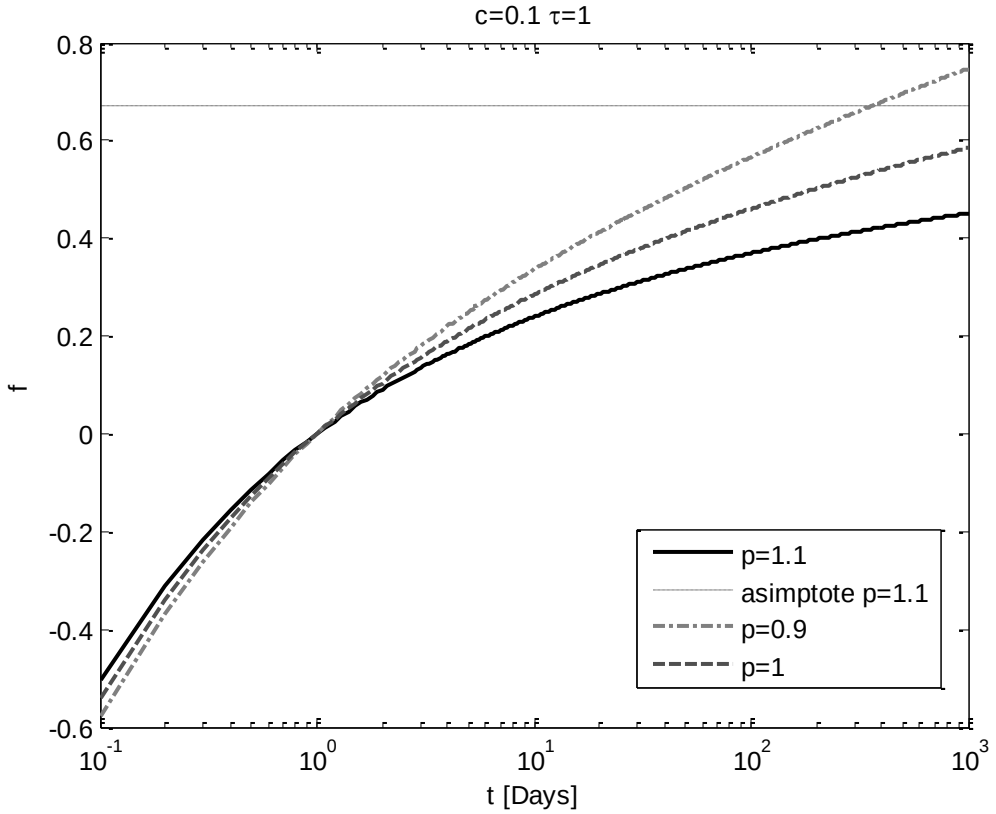

Fig. 1

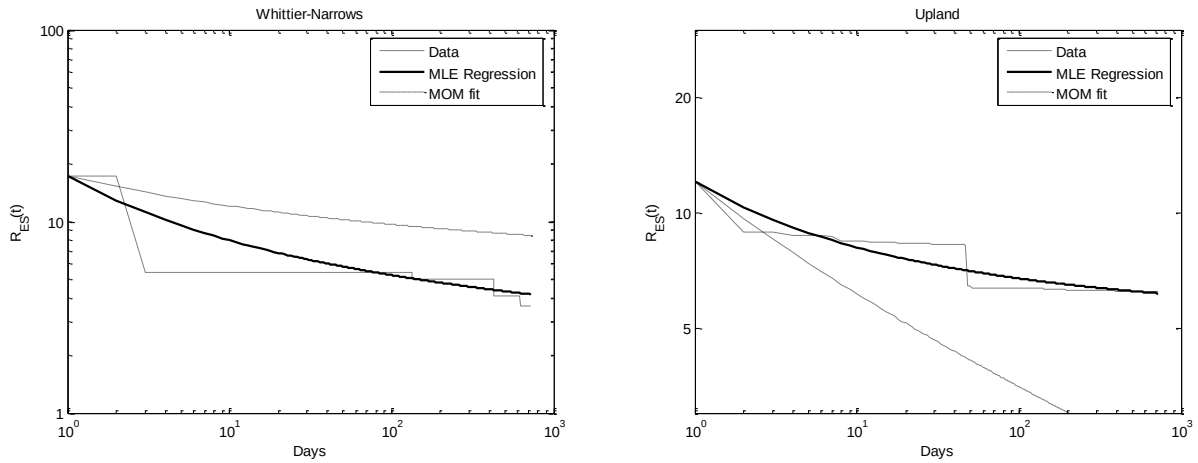

(a) (b)

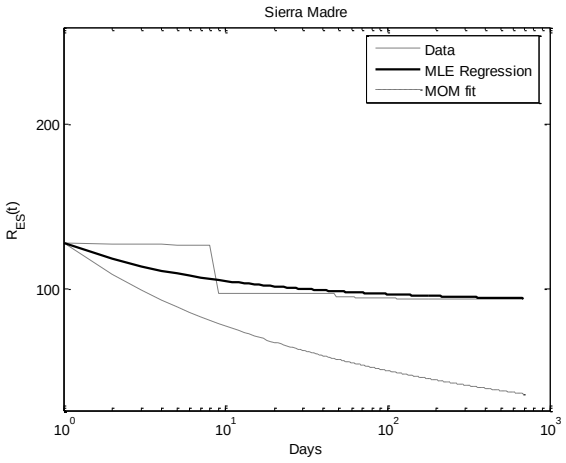

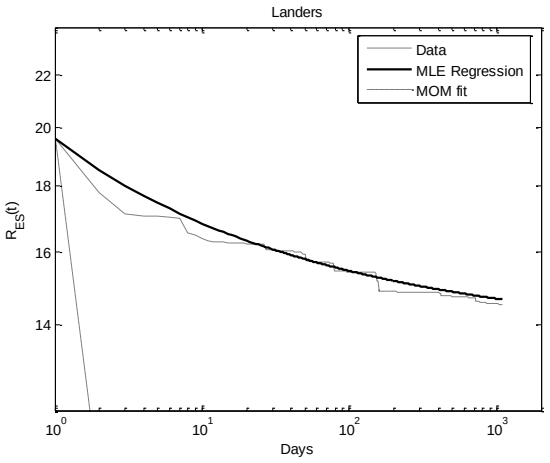

804

805 (c) (d)

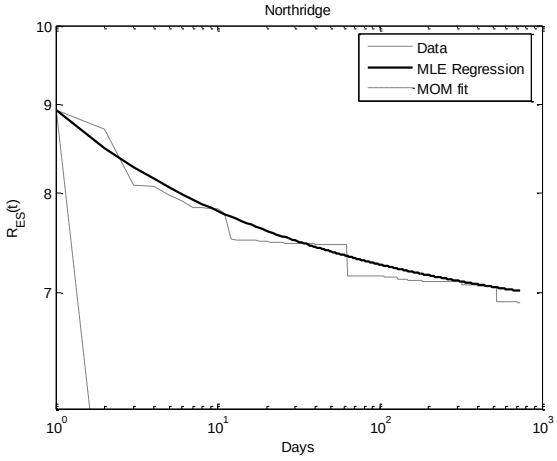

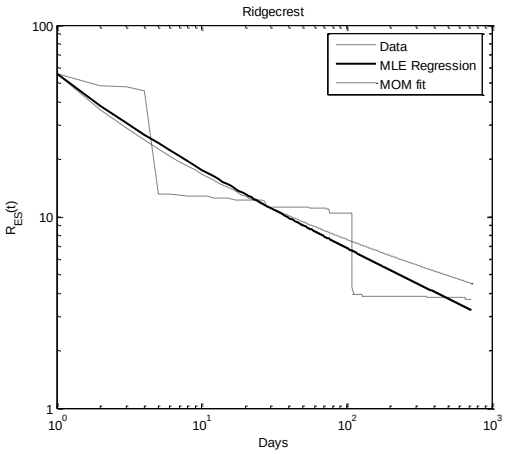

806

807 (e) (f)

808

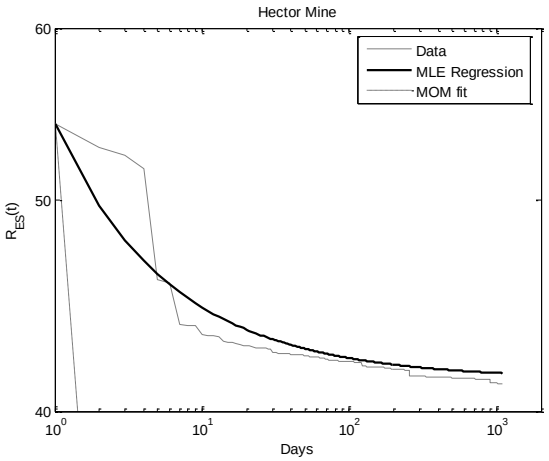

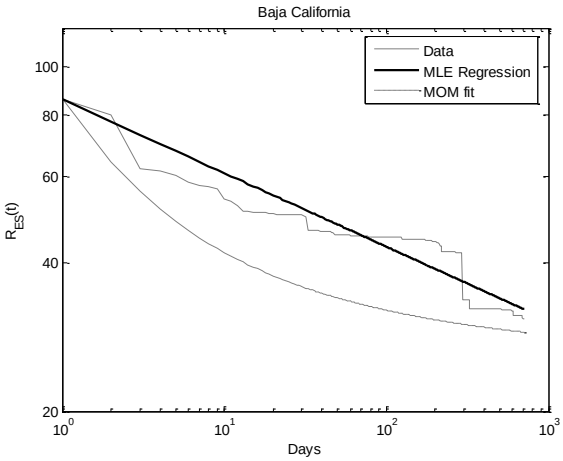

809

810 (g) (h)

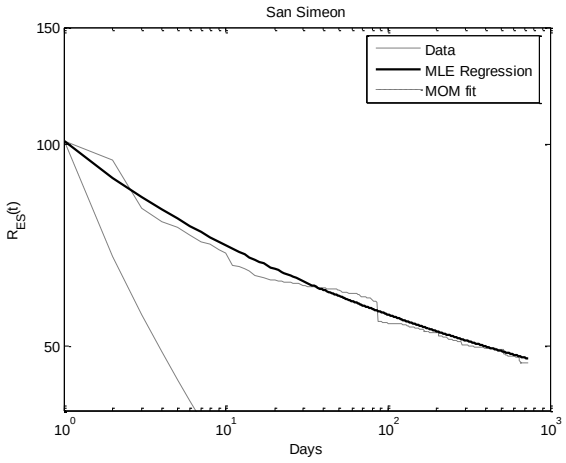

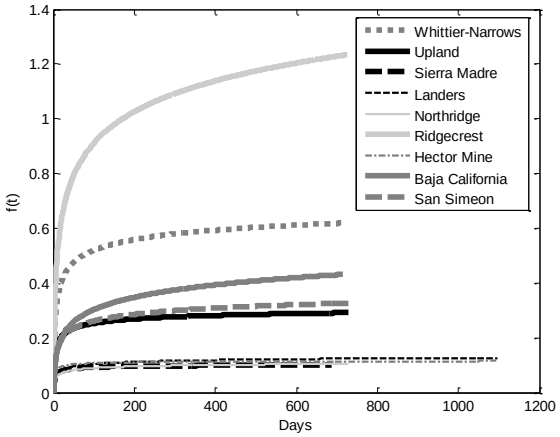

(i) (j)

Fig. 2

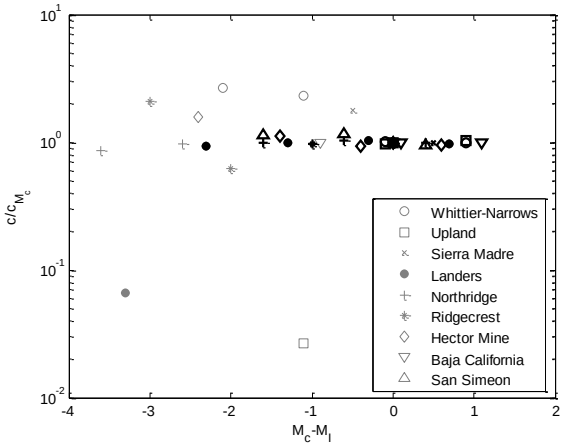

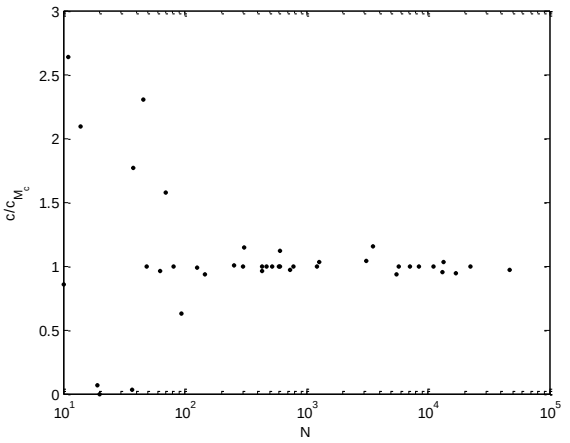

(a) (b)

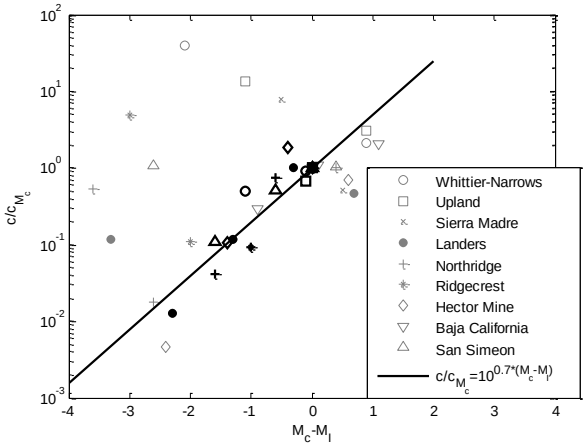

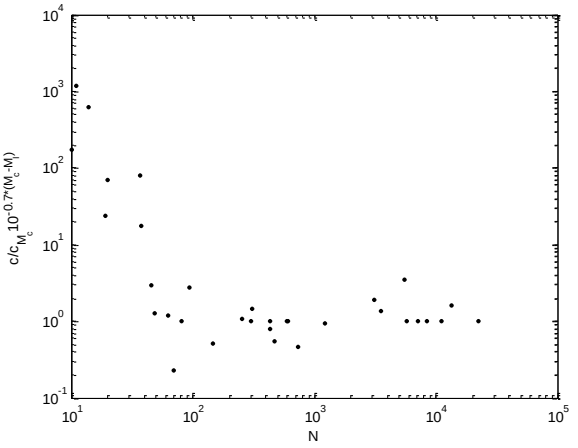

(c) (d)

Fig. 3

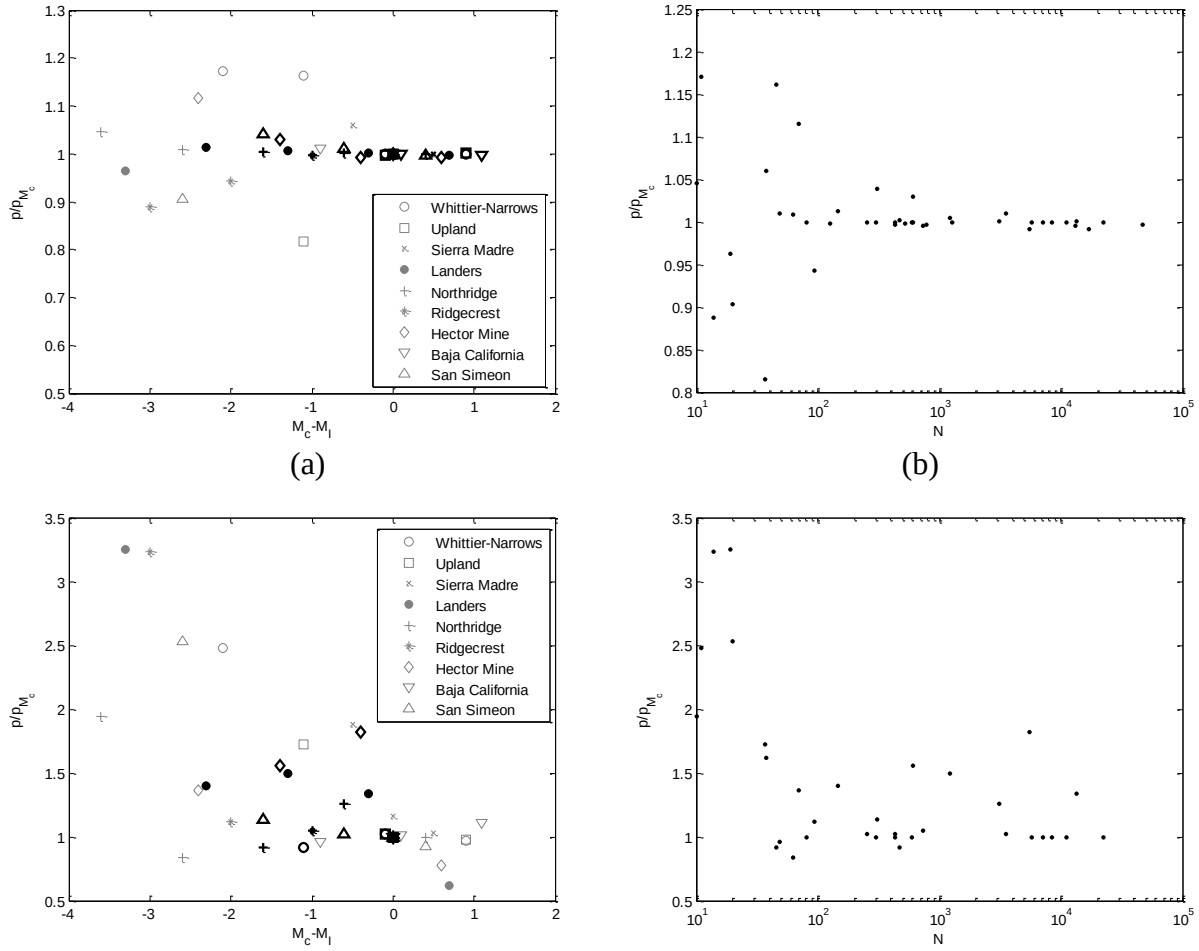
p/p_Mc
M_c-M_l
N
Whittier-Narrows
Upland
Sierra Madre
Landers
Northridge
Ridgecrest
Hector Mine
Baja California
San Simeon
(a)
(b)
(c)
(d)

Fig. 4

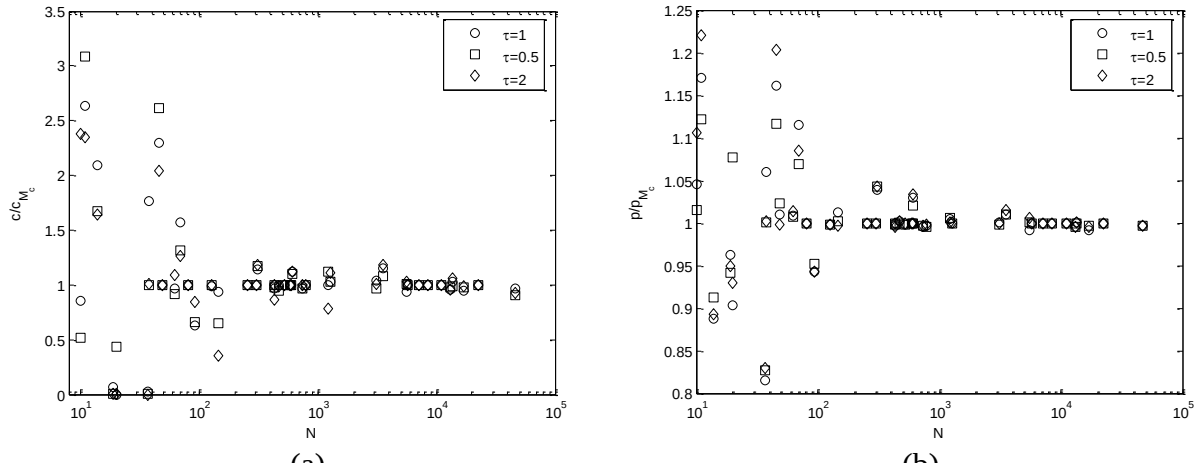
c/c_Mc
p/p_Mc
N
τ=1
τ=0.5
τ=2
(a)
(b)

Fig. 5

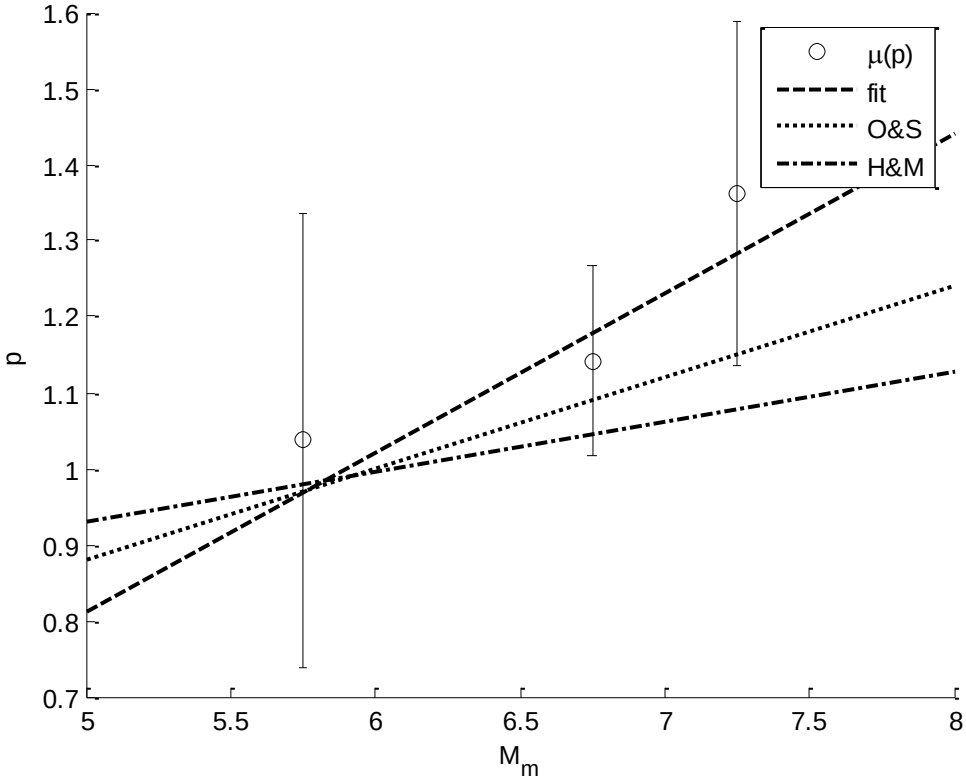

Fig. 6

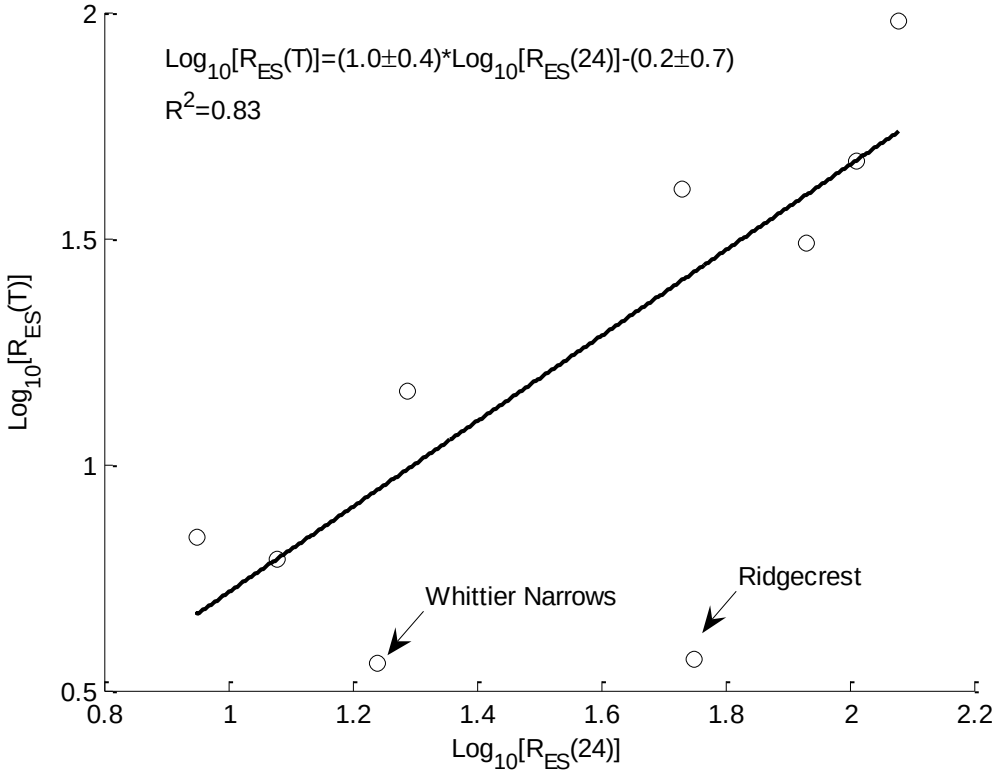
Log10[RES(T)]=(1.0±0.4)*Log10[RES(24)]-(0.2±0.7)
R2=0.83
Whittier Narrows
Ridgecrest
Log10[RES(T)]
Log10[RES(24)]
2
1.5
1
0.5
0.8
1
1.2
1.4
1.6
1.8
2
2.2

Fig. 7

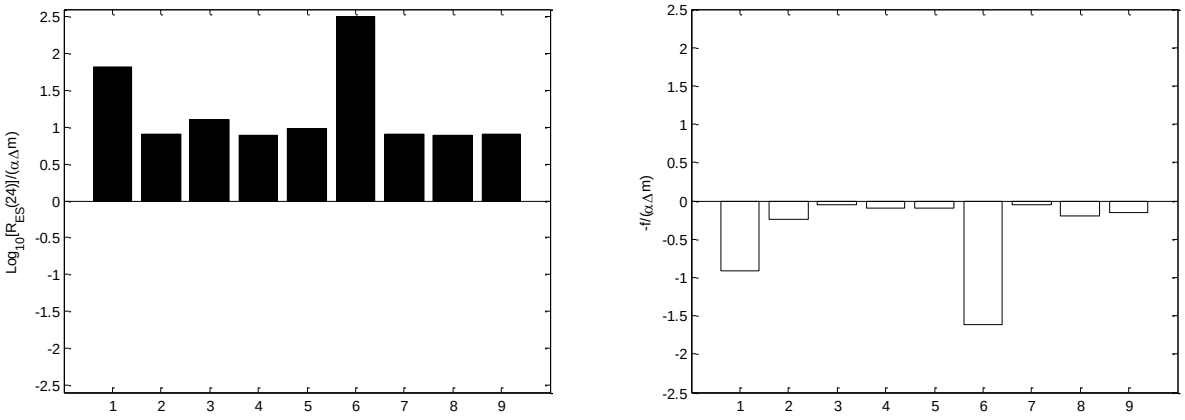
Log10[RES(24)]/(αΔm)
-f/(αΔm)

(a) (b)

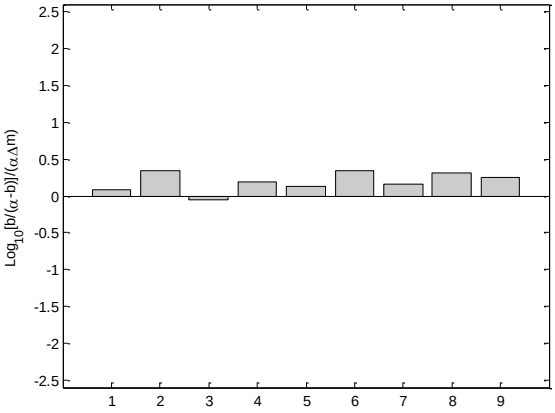
Log10[b/(α-b)]/(αΔm)
2.5
2
1.5
1
0.5
0
-0.5
-1
-1.5
-2
-2.5
1
2
3
4
5
6
7
8
9

(c)

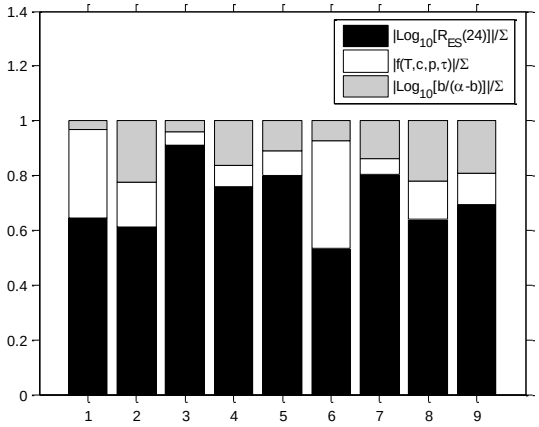
|Log10[RES(24)]|/Σ
|f(T,c,p,τ)|/Σ
|Log10[b/(α-b)]|/Σ
1.4
1.2
1
0.8
0.6
0.4
0.2
0
1
2
3
4
5
6
7
8
9

(d)

Fig. 8

Tables

N	Sequence	Main date yyyy/mm/dd	Lat	Lon	M_m	M_c	M_a	Aft date yyyy/mm/dd
1	Whittier Narrows	1987/10/01	34.061	-118.079	5.9	1.9±0.1	5.3	1987/10/04
2	Upland	1990/02/28	34.144	-117.697	5.5	1.9±0.08	4.7	1990/03/01
3	Sierra Madre	1991/06/28	34.270	-117.993	5.8	1.5±0.3	4.3	1991/06/28
4	Landers	1992/06/28	34.200	-116.437	7.3	1.7±0.06	6.3	1992/06/28
5	Northridge	1994/01/17	34.213	-118.537	6.7	1.4±0.1	5.9	1994/01/17
6	Ridgecrest	1995/09/20	35.761	-117.638	5.8	1.00±0.05	5.2	1996/01/07
7	Hector Mine	1999/10/16	34.594	-116.271	7.1	1.6±0.11	5.8	1999/10/16
8	Baja California	2002/02/22	32.319	-115.322	5.7	2.1±0.1	4.2	2002/12/12
9	San Simeon	2003/12/22	35.709	-121.104	6.5	1.4±0.03	4.7	2003/12/22

Table 1

N	Sequence	p	c	R^2	RMSE
1	Whittier Narrows	1.06±0.03	0.26±0.05	0.5056	0.0476
2	Upland	1.2±0.2	0.07±0.06	0.7110	0.0175
3	Sierra Madre	1.41± 0.05	0.03± 0.01	0.5737	0.0071
4	Landers	1.202± 0.002	0.00300±0.00002	0.8581	0.0046
5	Northridge	1.231± 0.009	0.0028±0.0002	0.7934	0.0051
6	Ridgecrest	0.65±0.02	0.13± 0.06	0.7280	0.0948
7	Hector Mine	1.52± 0.05	0.07± 0.01	0.6914	0.0042
8	Baja California	0.851± 0.005	0.0000±0.0000	0.8025	0.0341
9	San Simeon	1.05± 0.01	0.012±0.004	0.9676	0.0068

Table 2

parameters	R	t	Correlation s.l. 0.05
$Log_{10}(c/c_{Mc})$, M_c-M_I	-0.0999	0.3478	No correlation
p/pMc, Mc-MI	-0.0322	0.1116	No correlation
p, Mm (3 points)	0.9243	2.4217	Positive correlation
(9 points)	0.4529	1.3440	No correlation (positive with s.l. 0.15)
c, Mm	-0.3329	0.9340	No correlation (negative with s.l. 0.20)
p, c	-0.2314	0.6293	No correlation

Table 3

N	Sequence	$Log_{10}[R_{ES}(24)]$	f	$Log_{10}[b/(\alpha-b)]$	Theoretical Δm	Real Δm	$Log_{10}[R_{ES}(T)]$
1	Whittier Narrows	1.24	0.62	0.06	0.5	0.6	0.56
2	Upland	1.08	0.29	0.40	0.8	0.8	0.79
3	Sierra Madre	2.08	0.10	-0.09	1.3	1.5	1.98
4	Landers	1.29	0.13	0.28	1.0	1.0	1.16
5	Northridge	0.95	0.10	0.13	0.6	0.8	0.84
6	Ridgecrest	1.75	1.23	0.24	0.5	0.6	0.57
7	Hector Mine	1.73	0.11	0.30	1.3	1.3	1.61
8	Baja California	1.93	0.42	0.66	1.4	1.5	1.49
9	San Simeon	2.01	0.33	0.55	1.5	1.8	1.67
	Mean	1.56	0.37	0.28	1.0	1.1	1.18
	std	0.43	0.37	0.23	0.4	0.4	0.52

Table 4